

Acting Manager:

Dr. Mohammad Khansari
Assistant Professor
ICT Research Institute

Editor - In - Chief:

Dr. Kambiz Badie
Associate Professor
ICT Research Institute

Executive Manager:

Prof. Ahmad Khadem-Zadeh
Associate Professor
ICT Research Institute

Associate Editor (CT Section):

Dr. Reza Faraji-Dana
Professor
University of Tehran

Associate Editor (Network Section):

Dr. S. Majid Noorhoseini
Assistant Professor
Amirkabir University of Technology

Editorial Board:

Dr. Prof. Abdolali Abdipour
Professor
Amirkabir University of Technology

Dr. Hassan Aghaeinia
Associate Professor
Amirkabir University of Technology

Dr. Vahid Ahmadi
Professor
Tarbiat Modares University

Dr. Abbas Asosheh
Assistant Professor
Tarbiat Modares University

Dr. Karim Faez
Professor
Amirkabir University of Technology

Dr. Hossein Gharai
Assistant Professor
ICT Research Institute

Dr. Farrokh Hodjat Kashani
Professor
Iran University of Science & Technology

Dr. Ehsanollah Kabir
Professor
Tarbiat Modares University

Dr. Mahmoud Kamarei
Professor
University of Tehran

Dr. Manouchehr Kamyab
Associate Professor
K. N. Toosi University of Technology

Dr. Ghasem Mirjalili
Associate Professor
Yazd University

Dr. Kamal Mohamed-pour
Professor
K.N. Toosi University of Technology

Dr. Ali Moini
Associate Professor
University of Tehran

Dr. Ali Movaghar Rahimabadi
Professor
Sharif University of Technology

Dr. Keyvan Navi
Associate Professor
Shahid Beheshti University

Dr. Jalil Rashed Mohasel
Professor
University of Tehran

Dr. Babak Sadeghian
Associate Professor
Amirkabir University of Technology

Dr. S. Mostafa Safavi Hemami
Associate Professor
Amirkabir University of Technology

Dr. Ahmad Salahi
Associate Professor
ICT Research Institute

Dr. Hamid Soltanian-Zadeh
Professor
University of Tehran

Dr. Fattaneh Teghiyareh
Assistant Professor
University of Tehran

Dr. Mohammad Teshnehlab
Associate Professor
K. N. Toosi University of Technology

Dr. Mohammad Hossein Yaghmaee Moghaddam
Associate Professor
Ferdowsi University of Mashhad

Dr. Alireza Yari
Assistant Professor
ICT Research Institute

Secretariat Organizer:

Taha Sarhangi

Executive Assistants:

Valiollah Ghorbani
Nayereh Parsa-Shirin Mirzaie Ghazi



Topics of Interest

Information Technology

Information Systems

IT Applications & Services

IT Platforms: Software & Hardware Technology

IT Strategies & Frameworks

Communication Technology

Communication Devices

Communication Theory

Mobile Communications

Optical Communications

Satellite Communications

Signal / Image / Video Processing

Network Technology

Computer & Communication Networks

Wireless Networks

Network Management

Network Security

NGN Technology

Security Management

IJICTR

This Page intentionally left blank.



Spatial Interference Alignment in Relay-Assisted Multi-Cell Multi-User Networks

Ali Golestani

Department of Electrical Engineering
K.N. Toosi University of Technology
Tehran, Iran
agolestani@ee.kntu.ac.ir

Ali H. Bastami

Department of Electrical Engineering
K.N. Toosi University of Technology
Tehran, Iran
bastami@kntu.ac.ir

Kamal Mohamed-pour

Department of Electrical Engineering
K.N. Toosi University of Technology
Tehran, Iran
kmpour@kntu.ac.ir

Received: October 16, 2016- Accepted: December 27, 2016

Abstract—In this paper, the spatial interference alignment (IA) is investigated in the downlink (DL) of a relay-assisted multi-cell multi-user network. The transmission from the base station (BS) to the mobile station (MS) takes place in two phases with the help of the selected relay station (RS). The closed-form IA algorithms are employed in both the BS to RS and RS to MS links. The performance of this cooperative scheme is analyzed in terms of the sum rate and the sum degrees of freedom (DoF) for the amplify-and-forward (AF) and decode-and-forward (DF) relaying schemes. The simulation results of the sum rate show that the DF scheme significantly outperforms the noncooperative min-leakage and max-SINR iterative algorithms over the entire range of SNR, and the AF scheme performs very close to the min-leakage algorithm. Moreover, the DF scheme outperforms the noncooperative closed-form IA algorithm in the low and medium-SNR regimes.

Keywords- Cellular network, degrees of freedom, interference alignment, relay, sum rate.

I. INTRODUCTION

The co-channel interference has become the key challenge in the new generations of cellular communication networks that employ the frequency reuse factor (FRF) of unity. Especially, the inter-cell interference coming from the adjacent cells significantly diminishes the spectral efficiency of the cell-edge users. Implementing a smart interference management technique is a good solution to increase the spectral efficiency of the cell-edge users [1].

Interference alignment (IA) is a cooperative transmission and/or reception technique that can establish a high multiplexing gain by effectively decreasing the interference level in a multi-user system [2]. With the help of the IA technique, the multi-user interference channel can achieve its maximum degrees of freedom [3]. Therefore, in the high-SNR regime, the IA technique can make the sum-rate of the cellular system close to the sum-capacity of the system [4]. In a dense cellular network, some user terminals may be located in the coverage holes of the base station (BS). This situation is more probable for the cell-edge users. In these situations, utilizing the

relay nodes can be very helpful to improve the coverage area of the BS. The relay nodes can be selected among the idle nodes that are located in the coverage area of the BS, and the communications can be indirectly performed with the help of these intermediate nodes.

The combination of the cooperative communication schemes and the IA techniques is an appropriate way to simultaneously overcome the interference and fading impairments of the channel [5]-[10]. The problem of energy spectral efficiency maximization in the downlink (DL) of a multi-user multi-relay multi-cell time-division-duplex (TDD)-based network has been investigated in [5]. In [6], for a two-cell two-user relay-aided network, an IA scheme has been proposed in which the degrees of freedom can reach to its upper bound. The duality of the IA in the uplink (UL) and DL transmissions of a multi-cell multi-user relay-aided network with single-antenna users has been investigated in [7]. In [8], an enhanced relay-aided interference alignment (eRIA) scheme has been proposed in which a super relay is employed for the IA purposes between the BSs of a cellular network and their corresponding users. In [9] and [10], two IA-based two-hop protocols have been designed for the one-user-per-cell and two-user-per-cell scenarios, respectively, where the relay node and the cell-edge users are located at around the junction of the cells.

In this paper, the spatial IA is investigated in the DL of a relay-assisted multi-cell multi-user network. The transmission from the BS to the mobile station (MS) takes place in two hops with the help of the selected relay station (RS) which is chosen among the set of potential relay nodes. All the terminals of the network are equipped with multiple antennas. Accordingly, the first phase of transmission from the BSs to the selected RSs is modeled as a multiple-input multiple-output (MIMO) interfering broadcast channel (IFBC) and the second phase of transmission from the selected RSs to the MSs is modeled as a MIMO $K \times C$ -user interference channel, where C is the number of cells and K is the number of MSs per cell. In both phases of transmission, the closed-form IA algorithms are employed. The performance of this cooperative scheme is analyzed in terms of the sum rate and the sum degrees of freedom (DoF) for the amplify-and-forward (AF) and decode-and-forward (DF) relaying strategies. The simulation results of the sum rate show that the DF scheme significantly outperforms the noncooperative min-leakage and max-SINR iterative algorithms over the entire range of SNR, and the AF scheme performs very close to the min-leakage algorithm. Moreover, the DF scheme outperforms the noncooperative closed-form IA algorithm in the low and medium-SNR regimes. Also, the DoF analysis shows that the sum degrees of freedom in the first and second phases of the proposed schemes can achieve the optimal value under some special configurations.

The rest of this paper is organized as follows. Section II presents the system model and the protocol description. Section III analyzes the performance of the system in terms of the sum rate and the sum DoF. Section IV presents some simulation results and

numerical examples. Finally, Section V summarizes the main results of the paper.

Notation: We use boldface lowercase letters for vectors and boldface uppercase for matrices. $(\cdot)^T$ and $(\cdot)^H$ denote the transpose and the conjugate transpose, respectively. For the matrix \mathbf{A} , $\text{tr}(\mathbf{A})$ denotes the trace of \mathbf{A} , $\text{rank}(\mathbf{A})$ denotes the rank of \mathbf{A} , $\det(\mathbf{A})$ denotes the determinant of \mathbf{A} and $\lambda_i(\mathbf{A})$ denotes the i th largest eigenvalue of \mathbf{A} . $[a]^+ = \max(a, 0)$, $[a]$ denotes the smallest integer greater than or equal to a and $\lfloor a \rfloor$ denotes the largest integer less than or equal to a . \mathbb{C} represents the set of complex numbers. $a \equiv b$ is the remainder of the division of a by b .

II. SYSTEM MODEL AND PROTOCOL DESCRIPTION

In this section, we present the system model under investigation and the IA-based cooperative protocol.

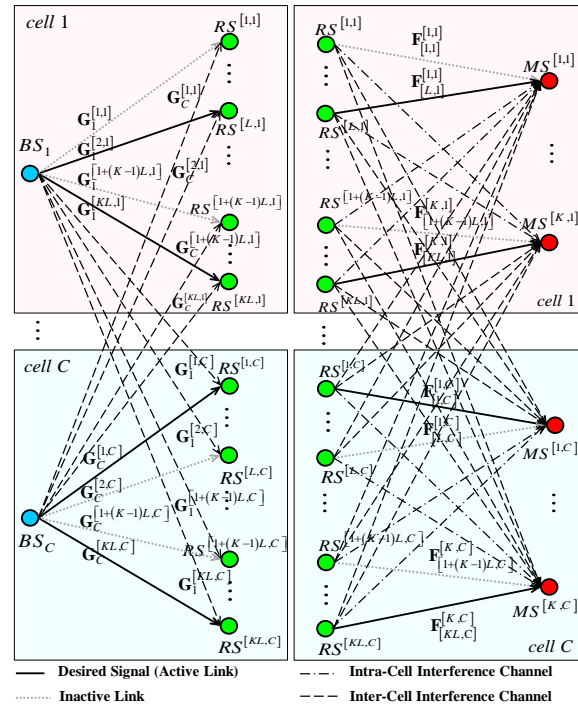


Fig. 1. System model

A. System Model

We consider a cellular network with C cells and the FRF of 1. Each cell consists of one BS located at the center of the cell, K MSs and $K \times L$ half-duplex RSs, as shown in Fig. 1. All the terminals operate over the same frequency band. The DL transmission from the BS to the MS is under investigation. It is assumed that there is no direct link between the BS and the MS, and hence, each MS receives the BS signal with the help of the selected RS which is chosen among L potential relay nodes. It is assumed that the BS and the MS are equipped with M_b and $N_{m,F}$ antennas, respectively, and each RS is equipped with M_r transmit and N_r receive antennas.

In Fig. 1, $RS^{[r,c]}$ and $MS^{[r,c]}$ denote the r th RS and MS of cell c , respectively. $\mathbf{G}_b^{[r,c]}$ is an $N_r \times M_b$ matrix that characterizes the MIMO channel from the BS of cell b to $RS^{[r,c]}$. Similarly, $\mathbf{F}_{[r,b]}^{[k,c]}$ is an $N_{m,F} \times M_r$ matrix that characterizes the MIMO channel from $RS^{[r,b]}$ to $MS^{[k,c]}$.



It is assumed that the wireless channels suffer from the frequency non-selective quasi-static fading plus shadowing [11] and additive white Gaussian noise (AWGN). Under Rayleigh fading assumption, each entry of the matrices $\mathbf{G}_b^{[r,c]}$ and $\mathbf{F}_{[r,b]}^{[k,c]}$ is a zero-mean circularly symmetric complex Gaussian random variable and the additive noise is distributed as $\mathcal{CN}(0, \sigma_n^2)$.

B. Protocol Description

1) **Relay Selection:** In the proposed scheme, the BS sends its message to the MS with the help of a single relay node. As described in the previous subsection, corresponding to each MS, there are L potential relay nodes. Thus, we should first select the best relay node based on an appropriate criterion. In this paper, we select the best relay node such that the minimum SNR of the BS-RS and RS-MS links is maximized [12]. This criterion can be formulated as

$$\text{rs}^{[k,c]} = \underset{1+L(k-1) \leq r \leq kL}{\text{argmax}} \min \left(\text{tr}(\mathbf{G}_c^{[r,c]} \mathbf{G}_c^{[r,c]H}), \text{tr}(\mathbf{F}_{[r,c]}^{[k,c]} \mathbf{F}_{[r,c]}^{[k,c]H}) \right) \quad (1)$$

$$\forall k \in \mathcal{K} \triangleq \{1, \dots, K\}; c \in \mathcal{C} \triangleq \{1, \dots, C\}$$

where $\text{rs}^{[k,c]}$ is the selected RS corresponding to $\text{MS}^{[k,c]}$. Considering all the interfering signals, we conclude that the first hop channel is a MIMO IFBC and the second hop channel is a MIMO $K \times C$ -user interference channel.

2) **First Phase:** In the first phase of the protocol, all the BSs transmit and the selected RSs listen. Let us focus on the signal transmitted by the BS of cell c . During the first hop, this BS transmits $d^{[r,c]}$ independent data streams to $\text{rs}^{[r,c]}$, where $d^{[r,c]} \leq \min\{M_b, N_r\}$, and for simplicity, we assume that $d^{[r,c]} = d, \forall r \in \mathcal{K}; c \in \mathcal{C}$. Under these circumstances, the configuration of the cellular network corresponding to the first hop of transmission can be described in a compact form as $(M_b \times (N_r, d)^K)^C$. Let $s_1^{[r,c]}, \dots, s_d^{[r,c]}$ denote the symbols transmitted by the BS to $\text{rs}^{[r,c]}$. By stacking the transmitted symbols in a $d \times 1$ vector, the transmitted signal can be described as $\mathbf{s}^{[r,c]} = [s_1^{[r,c]} \ s_2^{[r,c]} \ \dots \ s_d^{[r,c]}]^T$. It is assumed that $\mathbf{s}^{[r,c]}$ satisfies the power constraint $E\{\|\mathbf{s}^{[r,c]}\|^2\} \leq Pd$. As shown in Fig. 2, after applying the normalized and orthogonalized matrices of precoding $\mathbf{V}_G^{[r,c]} \in \mathbb{C}^{M_b \times d}$ and postcoding $\mathbf{U}_G^{[r,c]} \in \mathbb{C}^{N_r \times d}$, the effective received signal at $\text{rs}^{[r,c]}$ can be written as [13].

$$\begin{aligned} \hat{\mathbf{y}}_G^{[r,c]} &= \mathbf{U}_G^{[r,c]H} \mathbf{y}_G^{[r,c]} \\ &= \mathbf{U}_G^{[r,c]H} \mathbf{G}_c^{[r,c]} \mathbf{V}_G^{[r,c]} \mathbf{s}^{[r,c]} \\ &\quad + \mathbf{U}_G^{[r,c]H} \left(\sum_{\substack{\hat{r}=1, \hat{r} \neq r}}^K \mathbf{G}_c^{[r,c]} \mathbf{V}_G^{[\hat{r},c]} \mathbf{s}^{[\hat{r},c]} \right. \\ &\quad \left. + \sum_{b=1, b \neq c}^C \sum_{\hat{r}=1}^K \mathbf{G}_b^{[r,c]} \mathbf{V}_G^{[\hat{r},b]} \mathbf{s}^{[\hat{r},b]} \right) \\ &\quad + \hat{\mathbf{n}}_G^{[r,c]} \quad \forall r \in \mathcal{K}; c \in \mathcal{C} \end{aligned} \quad (2)$$

where $\mathbf{y}_G^{[r,c]}$ is the received signal at $\text{rs}^{[r,c]}$, $\hat{\mathbf{y}}_G^{[r,c]} \in \mathbb{C}^{d \times 1}$ and $\hat{\mathbf{n}}_G^{[r,c]} = \mathbf{U}_G^{[r,c]H} \mathbf{n}_G^{[r,c]}$, where $\mathbf{n}_G^{[r,c]}$ is the received noise vector at $\text{rs}^{[r,c]}$ and $\hat{\mathbf{n}}_G^{[r,c]}$ is distributed as $\mathcal{CN}(\mathbf{0}_{d \times 1}, \sigma_n^2 \mathbf{I}_d)$. The precoding and postcoding matrices are obtained based on the IA solution in [13]. In this case, in order to meet the feasibility condition of the IA, M_b and N_r must satisfy

$$\begin{aligned} M_b &= [K(C-1) + 1]d \\ N_r &= [(K-1)(C-1) + 1]d. \end{aligned} \quad (3)$$

Similar to the conventional MIMO IFBC scenario, we can define the signal and interference matrices, denoted by $\mathbf{S}_G^{[r,c]}$ and $\mathbf{J}_G^{[r,c]}$, as

$$\mathbf{S}_G^{[r,c]} \triangleq \sqrt{P} \mathbf{U}_G^{[r,c]H} \mathbf{G}_c^{[r,c]} \mathbf{V}_G^{[r,c]} \quad \forall r \in \mathcal{K}; c \in \mathcal{C} \quad (4)$$

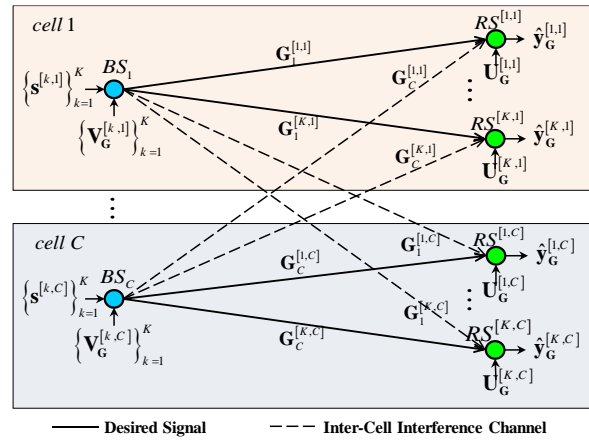


Fig. 2. System model corresponding to the first phase of the protocol. The precoding and postcoding matrices are applied to the $(M_b \times (N_r, d)^K)^C$ network.

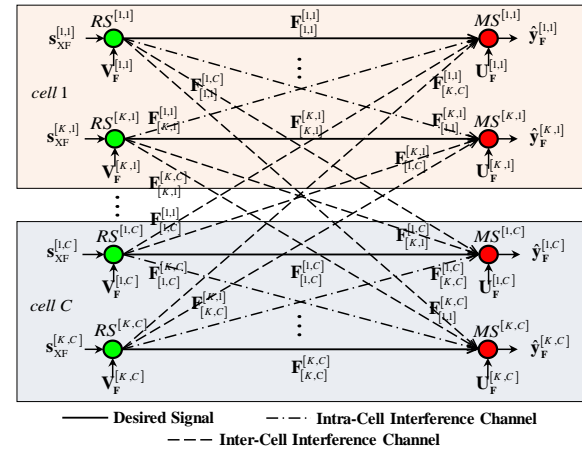


Fig. 3. System model corresponding to the second phase of the protocol. The precoding and postcoding matrices are applied to the $(M_r \times N_{m,F}, d)^{K \times C}$ network.

$$\begin{aligned} \mathbf{J}_G^{[r,c]} &\triangleq \sqrt{P} \mathbf{U}_G^{[r,c]H} \left[\left\{ \mathbf{G}_c^{[r,c]} \mathbf{V}_G^{[\hat{r},c]} \right\}_{\hat{r}=1, \hat{r} \neq r}^K \right. \\ &\quad \left. \left\{ \left\{ \mathbf{G}_b^{[r,c]} \mathbf{V}_G^{[\hat{r},b]} \right\}_{\hat{r}=1}^K \right\}_{b=1, b \neq c}^C \right] \\ &\quad \forall r \in \mathcal{K}; c \in \mathcal{C} \end{aligned} \quad (5)$$

where $\mathbf{S}_G^{[r,c]}$ is a $d \times d$ matrix representing the received desired signal by $\text{rs}^{[r,c]}$ and $\mathbf{J}_G^{[r,c]} \in \mathbb{C}^{d \times (KC-1)d}$ is the interference subspace matrix for this



relay node and is generated by putting $d \times d$ matrices of intra and inter-cell interference spaces together. In this case, the perfect IA conditions for $\mathbf{r}\mathbf{s}^{[r,c]}$ can be written as

$$\mathbf{J}_G^{[r,c]} = \mathbf{0}_{d \times (KC-1)d} \quad (6)$$

$$\text{rank}(\mathbf{S}_G^{[r,c]}) = d. \quad (7)$$

3) Second Phase: As mentioned earlier, in the second phase of the protocol, we have a MIMO $K \times C$ -user interference channel structure. The configuration of this network can be compactly described in its standard form as $(M_r \times N_{m,F}, d)^{K \times C}$. In the second phase, all the selected relay nodes transmit and the MSs listen. In this paper, we consider the AF and DF relaying schemes.

In the case of AF relaying, the transmitted signal by $\mathbf{r}\mathbf{s}^{[r,c]}$ can be described as

$$\mathbf{s}_{AF}^{[r,c]} = \omega_{AF}^{[r,c]} \hat{\mathbf{y}}_G^{[r,c]} \quad (8)$$

where $\hat{\mathbf{y}}_G^{[r,c]}$ is given in (2) and $\omega_{AF}^{[r,c]}$ is the amplification gain at $\mathbf{r}\mathbf{s}^{[r,c]}$ given by $\omega_{AF}^{[r,c]} = (P_{AF}^{[r,c]})^{1/2} / \|\hat{\mathbf{y}}_G^{[r,c]}\|$, where $P_{AF}^{[r,c]}$ denotes the transmitted power by $\mathbf{r}\mathbf{s}^{[r,c]}$.

In the case of DF relaying, the effective received signal at $\mathbf{r}\mathbf{s}^{[r,c]}$, i.e. $\mathbf{y}_G^{[r,c]}$, is first decoded and then re-encoded to form the transmitted signal $\mathbf{s}_{DF}^{[r,c]}$. It is assumed that $\mathbf{s}_{DF}^{[r,c]}$ satisfies the power constraint $E\{\|\mathbf{s}_{DF}^{[r,c]}\|^2\} \leq P_{DF}^{[r,c]}$.

As shown in Fig. 3, after applying the normalized and orthogonalized precoding and postcoding matrices, the effective received signal at $\mathbf{M}\mathbf{S}^{[k,c]}$ can be written as

$$\begin{aligned} \hat{\mathbf{y}}_F^{[k,c]} &= \mathbf{U}_F^{[k,c]H} \mathbf{y}_F^{[k,c]} \\ &= \mathbf{U}_F^{[k,c]H} \mathbf{F}_{[k,c]}^{[k,c]} \mathbf{V}_F^{[k,c]} \mathbf{s}_{XF}^{[k,c]} \\ &\quad + \mathbf{U}_F^{[k,c]H} \left(\sum_{r=1, r \neq k}^K \mathbf{F}_{[r,c]}^{[k,c]} \mathbf{V}_F^{[r,c]} \mathbf{s}_{XF}^{[r,c]} \right. \\ &\quad \left. + \sum_{b=1, b \neq c}^C \sum_{r=1}^K \mathbf{F}_{[r,b]}^{[k,c]} \mathbf{V}_F^{[r,b]} \mathbf{s}_{XF}^{[r,b]} \right) \\ &\quad + \hat{\mathbf{n}}_F^{[k,c]} \quad \forall k \in \mathcal{K}; c \in \mathcal{C} \end{aligned} \quad (9)$$

where $\mathbf{y}_F^{[k,c]}$ is the received signal at $\mathbf{M}\mathbf{S}^{[k,c]}$, $\mathbf{V}_F^{[r,c]} \in \mathbb{C}^{M_r \times d}$ and $\mathbf{U}_F^{[r,c]} \in \mathbb{C}^{N_{m,F} \times d}$ are the precoding and postcoding matrices, respectively, $\mathbf{s}_{XF}^{[r,c]}$ denotes either $\mathbf{s}_{AF}^{[r,c]}$ or $\mathbf{s}_{DF}^{[r,c]}$, and $\hat{\mathbf{n}}_F^{[k,c]}$ is given by

$$\hat{\mathbf{n}}_F^{[k,c]} = \mathbf{U}_F^{[k,c]H} \mathbf{n}_F^{[k,c]} \quad (10)$$

where $\mathbf{n}_F^{[k,c]}$ is the received noise vector at $\mathbf{M}\mathbf{S}^{[k,c]}$ and we have $\hat{\mathbf{n}}_F^{[k,c]} \sim \mathcal{CN}(\mathbf{0}_{d \times 1}, \sigma_n^2 \mathbf{I}_d)$. The precoding and postcoding matrices for the second phase of the protocol are obtained based on the closed-form IA algorithm [14] for the network $(M_r \times N_{m,F}, d)^{K \times C}$.

According to [14], the feasibility condition for the closed-form IA solution is given by

$$d < \min \left\{ \frac{N_{m,F}^2}{N_{m,F}KC - M_r}, \frac{N_{m,F} + M_r}{KC + 1} \right\}. \quad (11)$$

In the proposed AF and DF schemes, given that $KC \geq 3$ and $M_r > N_{m,F}$, $N_{m,F}$ and M_r that satisfy (11) can be calculated as

$$\begin{aligned} N_{m,F} &= \left\lfloor \frac{d}{2} \left[(KC + 1) - \sqrt{(KC + 1)(KC - 3)} \right] \right\rfloor \\ M_r &= \left\lfloor \frac{N_{m,F} \left(KC - \frac{N_{m,F}}{d} \right)}{\hat{M}} \right\rfloor \\ &\quad + \left(1 - \left\lfloor \frac{N_{m,F}^2}{N_{m,F}KC - \hat{M}} \right\rfloor \equiv d \right) \end{aligned} \quad (12)$$

and for the case that $KC \geq 3$ and $N_{m,F} > M_r$, M_r and $N_{m,F}$ can be obtained as

$$\begin{aligned} N_{m,F} &= \left\lfloor \frac{d}{2} \left[(KC + 1) + \sqrt{(KC + 1)(KC - 3)} \right] \right\rfloor \\ M_r &= \left\lfloor \frac{d(KC + 1) - \hat{N}}{\hat{M}} \right\rfloor \\ &\quad + \left(1 - \left\lfloor \frac{N_{m,F}^2}{N_{m,F}KC - \hat{M}} \right\rfloor \equiv d \right). \end{aligned} \quad (13)$$

Assuming $P_{AF}^{[r,c]} = P_{DF}^{[r,c]} = Pd$, the signal and interference matrices corresponding to the second hop transmission can be defined as

$$\mathbf{S}_F^{[k,c]} = \sqrt{P} \mathbf{U}_F^{[k,c]H} \mathbf{F}_{[k,c]}^{[k,c]} \mathbf{V}_F^{[k,c]} \quad \forall k \in \mathcal{K}; c \in \mathcal{C} \quad (14)$$

$$\begin{aligned} \mathbf{J}_F^{[k,c]} &= \sqrt{P} \mathbf{U}_F^{[k,c]H} \left[\left\{ \mathbf{F}_{[r,c]}^{[k,c]} \mathbf{V}_F^{[r,c]} \right\}_{r=1, r \neq k}^K \right. \\ &\quad \left. \left\{ \mathbf{F}_{[r,b]}^{[k,c]} \mathbf{V}_F^{[r,b]} \right\}_{r=1}^K \right]_{b=1, b \neq c}^C \\ &\quad \forall k \in \mathcal{K}; c \in \mathcal{C} \end{aligned} \quad (15)$$

Based on the above matrices, the perfect IA conditions for the second phase of the protocol can be described as

$$\mathbf{J}_F^{[k,c]} = \mathbf{0}_{d \times (KC-1)d} \quad \forall k \in \mathcal{K}; c \in \mathcal{C} \quad (16)$$

$$\text{rank}(\mathbf{S}_F^{[k,c]}) = d \quad \forall k \in \mathcal{K}; c \in \mathcal{C}. \quad (17)$$

III. PERFORMANCE ANALYSIS

In this section, we analyze the performance of the system in terms of the sum rate and the sum DoF.

A. AF Scheme

For the case of the AF scheme, the achievable rate at $\mathbf{M}\mathbf{S}^{[k,c]}$ can be calculated as

$$R_{AF}^{[k,c]} = \frac{1}{2} \log_2 \left(\det \left[\mathbf{I}_d + \boldsymbol{\Psi}_{AF}^{[k,c]} \right] \right) \quad (18)$$

where $\boldsymbol{\Psi}_{AF}^{[k,c]}$ is the $d \times d$ matrix of the received signal-to-interference-plus-noise ratio (SINR) at $\mathbf{M}\mathbf{S}^{[k,c]}$ and is given by

$$\boldsymbol{\Psi}_{AF}^{[k,c]} = \boldsymbol{\Psi}_G^{[k,c]} \boldsymbol{\Psi}_F^{[k,c]} \left(\mathbf{I}_d + \boldsymbol{\Psi}_G^{[k,c]} + \boldsymbol{\Psi}_F^{[k,c]} \right)^{-1} \quad (19)$$



where $\Psi_G^{[k,c]}$ and $\Psi_F^{[k,c]}$ are the $d \times d$ matrices of the SINR corresponding to the first and second phases of the protocol, respectively. These two matrices can be calculated as

$$\Psi_G^{[k,c]} = \mathbf{S}_G^{[k,c]} \mathbf{S}_G^{[k,c]H} \left(\sigma_n^2 \mathbf{I}_d + \mathbf{J}_G^{[k,c]} \mathbf{J}_G^{[k,c]H} \right)^{-1} \quad (20)$$

$$\Psi_F^{[k,c]} = \mathbf{S}_F^{[k,c]} \mathbf{S}_F^{[k,c]H} \left(\sigma_n^2 \mathbf{I}_d + \mathbf{J}_F^{[k,c]} \mathbf{J}_F^{[k,c]H} \right)^{-1} \quad (21)$$

In (18), the factor 1/2 reflects the half-duplex limitation of the relay nodes. By summing the achievable rates over all users and cells, the achievable sum-rate for the IA-based cellular system with AF relaying can be obtained as

$$\begin{aligned} R_{AF}^\Sigma &= \sum_{c=1}^C \sum_{k=1}^K R_{AF}^{[k,c]} \\ &= \frac{1}{2} \sum_{c=1}^C \sum_{k=1}^K \log_2 \left(\det[\mathbf{I}_d + \Psi_{AF}^{[k,c]}] \right). \end{aligned} \quad (22)$$

Appendix A calculates (22) in detail.

The sum DoF, denoted by \hat{d}_{AF}^Σ , can be easily calculated in terms of the sum rate as

$$\begin{aligned} \hat{d}_{AF}^\Sigma &= \lim_{P \rightarrow \infty} \frac{R_{AF}^\Sigma}{\log_2(P)} \\ &= \frac{1}{2} \lim_{P \rightarrow \infty} \sum_{c=1}^C \sum_{k=1}^K \frac{\log_2 \left(\det[\mathbf{I}_d + \Psi_{AF}^{[k,c]}] \right)}{\log_2(P)}. \end{aligned} \quad (23)$$

B. DF Scheme

Similar to the AF case, for the DF scheme, the achievable rate at $MS^{[k,c]}$ can be expressed as

$$R_{DF}^{[k,c]} = \frac{1}{2} \log_2 \left(\det[\mathbf{I}_d + \Psi_{DF}^{[k,c]}] \right) \quad (24)$$

where $\Psi_{DF}^{[k,c]}$ is the matrix of the received SINR at $MS^{[k,c]}$, which can be calculated as

$$\Psi_{DF}^{[k,c]} = \left(\sigma_n^2 \mathbf{I}_d + \mathbf{J}_F^{[k,c]} \mathbf{J}_F^{[k,c]H} \right)^{-1} \mathbf{S}_F^{[k,c]} \mathbf{S}_F^{[k,c]H}. \quad (25)$$

By summing $R_{DF}^{[k,c]}$ over k and c , the achievable sum rate for the IA-based cellular system with DF relaying can be computed as

$$\begin{aligned} R_{DF}^\Sigma &= \sum_{c=1}^C \sum_{k=1}^K R_{DF}^{[k,c]} \\ &= \frac{1}{2} \sum_{c=1}^C \sum_{k=1}^K \log_2 \left(\det[\mathbf{I}_d + \Psi_{DF}^{[k,c]}] \right). \end{aligned} \quad (26)$$

Appendix B calculates (26) in detail.

Using R_{DF}^Σ , the sum DoF can be calculated as

$$\hat{d}_{DF}^\Sigma = \lim_{P \rightarrow \infty} \frac{R_{DF}^\Sigma}{\log_2(P)}. \quad (27)$$

Substituting (26) into (27), after some manipulations, the sum DoF can be obtained as

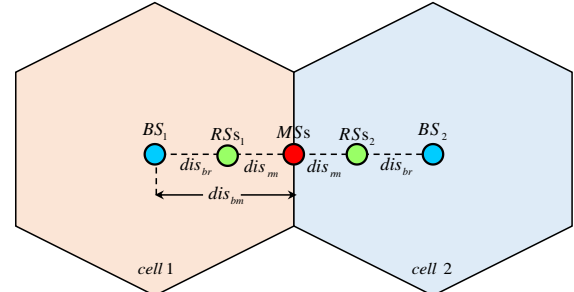


Fig. 4. Position of the nodes in a two-cell network. In each cell, there are two co-located cell-edge MSs, and corresponding to each MS, there are three co-located RSs.

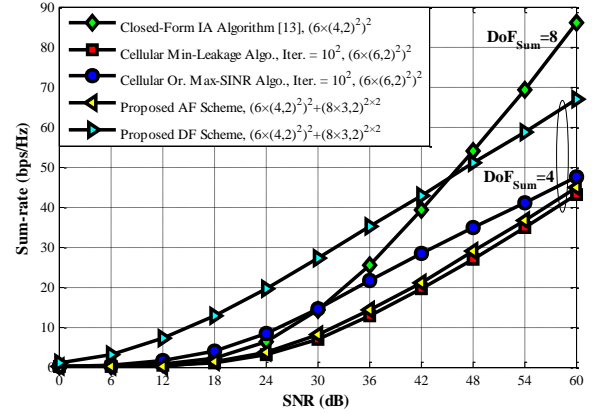


Fig. 5. Comparison of the sum rate in a two-cell network with $K = 2$, $L = 3$, $d = 2$ and for the first scenario. The path-loss exponent equals 3.5.

$$\begin{aligned} \hat{d}_{DF}^\Sigma &= \sum_{c=1}^C \sum_{k=1}^K \hat{d}_{DF}^{[k,c]} \\ &= \sum_{c=1}^C \sum_{k=1}^K \frac{1}{2} \left[\text{rank}(\mathbf{S}_F^{[k,c]}) - \text{rank}(\mathbf{J}_F^{[k,c]}) \right]^+. \end{aligned} \quad (28)$$

The proof is given in Appendix C.

IV. SIMULATION RESULTS

In this section, some numerical examples on the performance of the proposed schemes are presented. We also compare the proposed schemes with the IA-based noncooperative schemes in terms of the sum-rate and the sum DoF. In the noncooperative schemes, for the IA purposes, we consider the cellular min-leakage algorithm [16], the cellular orthogonalized max-SINR algorithm [16], and the closed-form IA solution [13].

A. General Assumptions

Throughout the simulations, it is assumed that $\sigma_n^2 = 1$ and $M_r > N_{m,F}$. In Figs. 5, 7, 9 and 12, the path-loss exponent equals 3.5 and in Figs. 6, 8, 10 and 13, the path-loss exponent equals 5. In the figures, SNR is defined as P_T/σ_n^2 , where P_T denotes the power allocated to each BS. Thus, the power allocated to each transmitted symbol is given as $P(i) =$



$10^{P_T(i)/10}/Kd$. It is also assumed that $P_{AF}(i) = P_{DF}(i) = P(i)d$, $C = 2$, $K = 2$ and $L = 3$. To have a fair comparison with the noncooperative schemes, the total transmitted power by the BS and the RS in the relay-assisted schemes is assumed to be equal to the transmitted power by the BS in the noncooperative schemes.

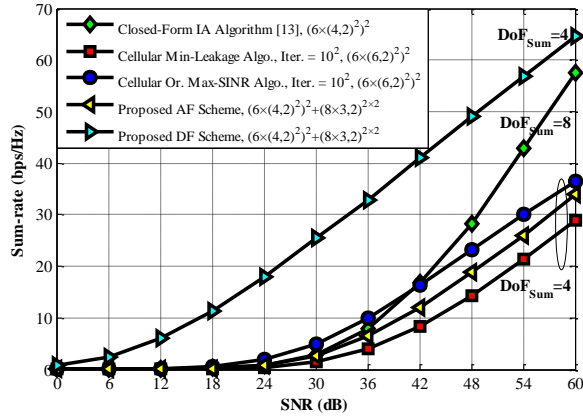


Fig. 6. Comparison of the sum rate in a two-cell network with $K = 2$, $L = 3$, $d = 2$ and for the first scenario. The path-loss exponent equals 5.

B. First Scenario

Let $h_{i,j}$ denote the channel coefficient from terminal i to terminal j . It is assumed that $h_{i,j} \sim \mathcal{CN}(0, \sigma_{i,j}^2)$, where $\sigma_{i,j}^2$ is given by

$$\sigma_{i,j}^2 = (\text{dis}_{i,j}/\text{dis}_0)^{-\gamma} \quad (29)$$

where $\text{dis}_{i,j}$ denotes the distance between terminals i and j , dis_0 is a fixed reference distance and γ is the path-loss exponent. Let $\text{dis}_{b,MS}^{[k,c]}$, $\text{dis}_{b,RS}^{[r,c]}$ and $\text{dis}_{r,b}^{[k,c]}$ denote the distance between the BS of cell b and $MS^{[k,c]}$, the distance between the BS of cell b and $RS^{[r,c]}$, and the distance between $RS^{[r,b]}$ and $MS^{[k,c]}$, respectively. It is assumed that

$$\begin{aligned} \text{dis}_{b,MS}^{[k,c]} &= \text{dis}_{bm} = 5 \text{dis}_0 \quad \forall k \in \mathcal{K}; b, c \in \mathcal{C} \\ \text{dis}_{b,RS}^{[r,c]} &= \text{dis}_{br} \quad \forall r \in \mathcal{K}; b, c \in \mathcal{C} \\ \text{dis}_{r,b}^{[k,c]} &= \text{dis}_{rm} \quad \forall r, k \in \mathcal{K}; b, c \in \mathcal{C} \\ \text{dis}_{bm} &= \text{dis}_{br} + \text{dis}_{rm}. \end{aligned} \quad (30)$$

Fig. 4 shows the network geometry under investigation. In this figure, it is assumed that $\text{dis}_{br} = 0.75\text{dis}_0$. Figs. 5 and 6 depict the sum rate performance of the proposed schemes as a function of SNR under the above assumptions and for the case that $d = 2$. The sum DoF corresponding to each scheme has been also shown in these figures. From Figs. 5 and 6, we observe that the AF scheme performs very close to the min-leakage algorithm over the entire range of SNR. We also observe that the DF scheme significantly outperforms both the min-leakage and max-SINR algorithms over the entire range of SNR. Also, the DF scheme outperforms the closed-form algorithm for the low and medium values of SNR. From Figs. 5 and 6, we also observe that the sum rate versus SNR curves in the AF and DF schemes and the iterative algorithms have the same slope in the high-SNR regime. This observation

implies that these schemes achieve the same sum DoF. This observation is in agreement with the DoF values shown in the figures.

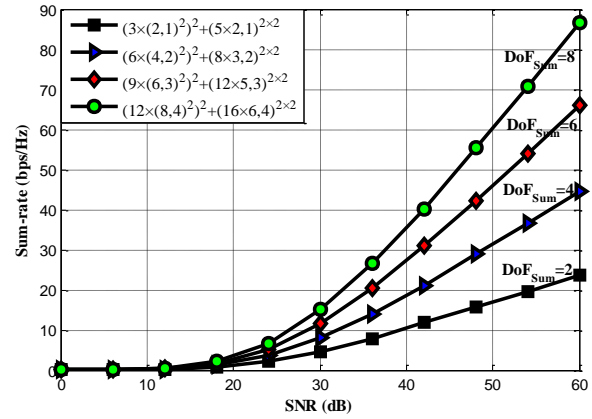


Fig. 7. Sum rate of the proposed AF scheme for different number of transmitted data streams $d = 1, \dots, 4$ in a two-cell system with $K = 2$ and $L = 3$. The path-loss exponent equals 3.5.

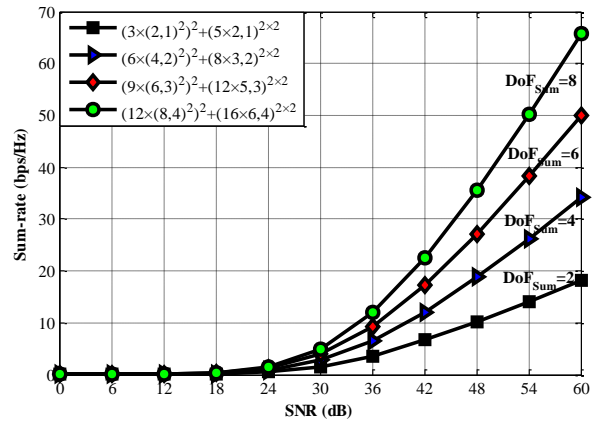


Fig. 8. Sum rate of the proposed AF scheme for different number of transmitted data streams $d = 1, \dots, 4$ in a two-cell system with $K = 2$ and $L = 3$. The path-loss exponent equals 5.

As shown in Figs. 5 and 6, under perfect IA conditions, the sum DoFs in the closed-form IA solution [13] and the iterative algorithms are equal to $\hat{d}_\Sigma = KC\hat{d} = KCd = 8$ and $\hat{d}_\Sigma = KC\hat{d} = \frac{1}{2}KCd = 4$, respectively. On the other hand, the maximum achievable DoF for the $(M_b \times (N_{m,H}, d)^K)^C$ MIMO-IFBC can be calculated as [4], [17]

$$d_\Sigma = \min\{CM_b, KCN_{m,H}, \max(M_b, KN_{m,H})\}. \quad (31)$$

Therefore, the algorithm in [13] and the iterative algorithms must achieve $d_\Sigma = KN_{m,H} = 8$ and $d_\Sigma = KN_{m,H} = CM_b = 12$ under the configurations of $(6 \times (4,2)^2)^2$ and $(6 \times (6,2)^2)^2$, respectively. Also, under perfect IA conditions, the first and second phases of the proposed schemes are able to achieve $\hat{d}_\Sigma = KCd = 8$ degrees of freedom. The maximum achievable DoF for the first phase of the proposed schemes under the configuration of $(6 \times (4,2)^2)^2$ can be calculated as $d_\Sigma = \min\{CM_b, KCN_r, \max(M_b, KN_r)\} = KN_r = 8$. On the other hand, the maximum achievable DoF for the $(M_r \times N_{m,F}, d)^{K \times C}$ $K \times C$ -user MIMO interference channel can be computed as [18]



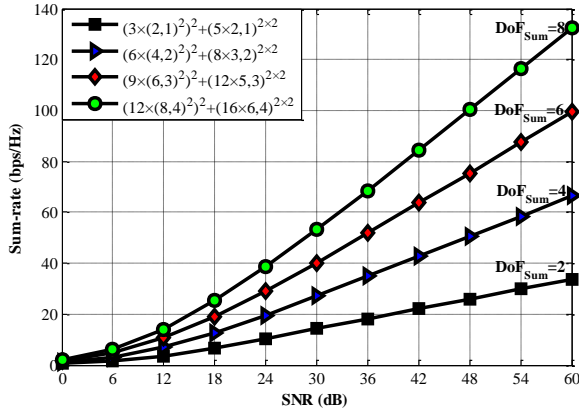


Fig. 9. Sum rate of the proposed DF scheme for different number of transmitted data streams $d = 1, \dots, 4$ in a two-cell system with $K = 2$ and $L = 3$. The path-loss exponent equals 3.5.

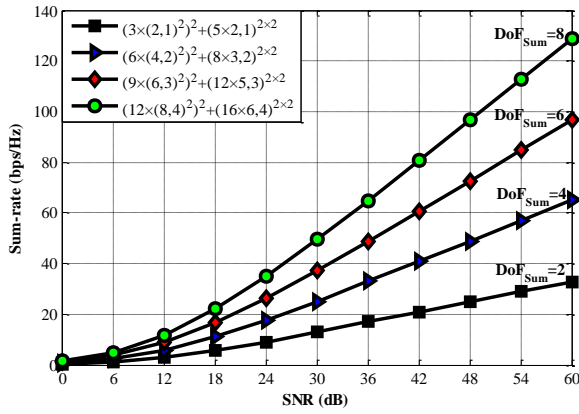


Fig. 10. Sum rate of the proposed DF scheme for different number of transmitted data streams $d = 1, \dots, 4$ in a two-cell system with $K = 2$ and $L = 3$. The path-loss exponent equals 5.

$$d_{\Sigma} = \begin{cases} \min(M_r, N_{m,F})KC, & KC \leq r \\ \min(M_r, N_{m,F})\frac{r}{r+1}KC, & KC > r \end{cases} \quad (32)$$

where $r = \lfloor \max(M_r, N_{m,F}) / \min(M_r, N_{m,F}) \rfloor$. Accordingly, the maximum achievable DoF for the second phase of the proposed schemes under the configuration of $(8 \times 3, 2)^{2 \times 2}$ equals $d_{\Sigma} = KC \min(M_r, N_{m,F})r / (r + 1) = 8$. Based on the above DoF analysis, among these schemes, the closed-form IA algorithm [13] and also the first and second phases of the AF and DF schemes can achieve the optimal DoF.

Figs. 7–10 illustrate the performance of the AF and DF schemes for different number of transmitted data streams in terms of the sum rate and the sum DoF. According to these figures, as the number of transmitted data streams increases, the sum DoF in the proposed schemes grows linearly. Thus, the sum rate of the proposed schemes is expected to increase linearly in the high-SNR regime.

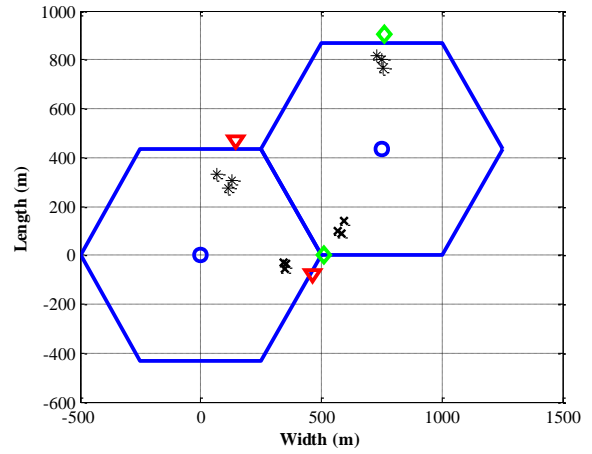


Fig. 11. Wrap-around-cell layout in a distributed two-cell network with radius 500m. In each cell, there are two cell-edge MSs, and corresponding to each MS, there are three RSs.

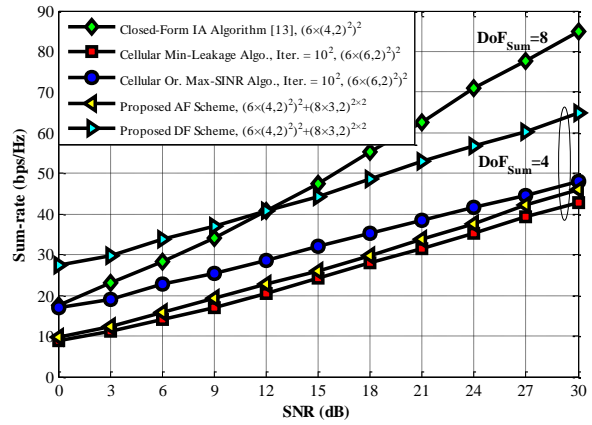


Fig. 12. Comparison of the sum rate performance in a two-cell system with $K = 2$, $L = 3$, $d = 2$ and for the second scenario. The path-loss exponent equals 3.5.

C. Second Scenario

In this scenario, $\sigma_{i,j}^2$ is chosen as [11]

$$\sigma_{i,j}^2 = A\psi(\text{dis}_{i,j}/\text{dis}_0)^{-\gamma} \quad (33)$$

where ψ is a random variable with variance σ_{SF}^2 representing the log-normal shadowing and A is an appropriate constant. We assume that $\sigma_{SF} = 8$ dB, and the wrap-around-cell layout shown in Fig. 11 is considered for the network geometry. Figs. 12 and 13 compare the performance of the abovementioned schemes in terms of the sum rate and the sum DoF for the second scenario.

By comparing Figs. 5, 7, 9, 12 and Figs. 6, 8, 10, 13, we observe that as the path-loss exponent increases, the performance of all the schemes degrades. However, the proposed schemes exhibit a more robust behavior comparing to the noncooperative schemes.

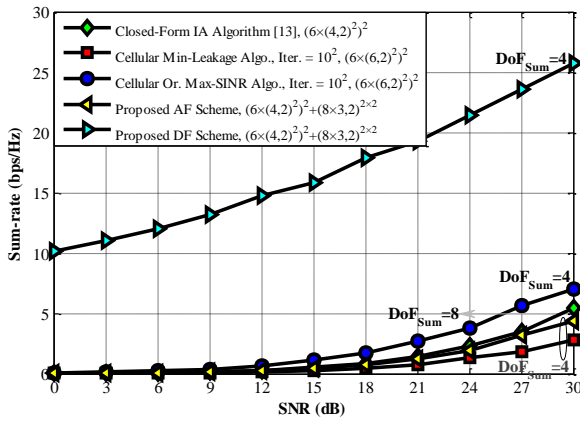


Fig. 13. Comparison of the sum rate performance in a two-cell system with $K = 2$, $L = 3$, $d = 2$ and for the second scenario. The path-loss exponent equals 5.

V. CONCLUSION

In this paper, the spatial IA was investigated in the DL of a relay-assisted multi-cell multi-user network. The performance of this system was analyzed in terms of the sum rate and the sum DoF for the AF and DF relaying schemes. The simulation results showed that the DF scheme significantly outperforms the noncooperative min-leakage and max-SINR iterative algorithms over the entire range of SNR. Moreover, the DF scheme outperforms the noncooperative closed-form IA algorithm in the low and medium-SNR regimes. The DoF performance of the system also showed that the relay-assisted schemes can effectively eliminate the inter-cell and intra-cell types of interference.

APPENDIX A CALCULATION OF (22)

Assuming i.i.d. Gaussian signaling, the achievable sum-rate for the AF scheme given in (22) can be rewritten as

$$R_{AF}^{\Sigma} = \frac{1}{2} \sum_{c=1}^C \sum_{k=1}^K \sum_{i=1}^d \log_2 \left(1 + \Psi_{i,AF}^{[k,c]} \right) \quad (34)$$

where $\Psi_{i,AF}^{[k,c]}$ is given by

$$\Psi_{i,AF}^{[k,c]} = \frac{\Psi_{i,G}^{[k,c]} \Psi_{i,F}^{[k,c]}}{1 + \Psi_{i,G}^{[k,c]} + \Psi_{i,F}^{[k,c]}} \quad (35)$$

$\Psi_{i,G}^{[k,c]}$ and $\Psi_{i,F}^{[k,c]}$ are the SINRs of the i th received stream corresponding to the first and second phases of the protocol, respectively. These two SINR values can be calculated as

$$\begin{aligned} \Psi_{i,G}^{[k,c]} &= P \left| \mathbf{u}_{i,G}^{[k,c]H} \mathbf{G}_c^{[k,c]} \mathbf{v}_{i,G}^{[k,c]} \right|^2 \\ &\div \left(\sigma_n^2 + \sum_{j=1, j \neq i}^d P \left| \mathbf{u}_{i,G}^{[k,c]H} \mathbf{G}_c^{[k,c]} \mathbf{v}_{j,G}^{[k,c]} \right|^2 \right. \\ &\quad \left. + \sum_{r=1, r \neq k}^K \sum_{j=1}^d P \left| \mathbf{u}_{i,G}^{[k,c]H} \mathbf{G}_c^{[k,c]} \mathbf{v}_{j,r}^{[k,c]} \right|^2 \right) \end{aligned} \quad (36)$$

$$+ \sum_{b=1, b \neq c}^C \sum_{r=1}^K \sum_{j=1}^d P \left| \mathbf{u}_{i,G}^{[k,c]H} \mathbf{G}_b^{[k,c]} \mathbf{v}_{j,r}^{[k,c]} \right|^2 \Bigg)$$

and the sum DoF for the AF and DF relaying

$$\begin{aligned} \Psi_{i,F}^{[k,c]} &= P \left| \mathbf{u}_{i,F}^{[k,c]H} \mathbf{F}_{[k,c]}^{[k,c]} \mathbf{v}_{i,F}^{[k,c]} \right|^2 \\ &\div \left(\sigma_n^2 + \sum_{j=1, j \neq i}^d P \left| \mathbf{u}_{i,F}^{[k,c]H} \mathbf{F}_{[k,c]}^{[k,c]} \mathbf{v}_{j,F}^{[k,c]} \right|^2 \right. \\ &\quad \left. + \sum_{r=1, r \neq k}^K \sum_{j=1}^d P \left| \mathbf{u}_{i,F}^{[k,c]H} \mathbf{F}_{[r,c]}^{[k,c]} \mathbf{v}_{j,r}^{[k,c]} \right|^2 \right. \\ &\quad \left. + \sum_{b=1, b \neq c}^C \sum_{r=1}^K \sum_{j=1}^d P \left| \mathbf{u}_{i,F}^{[k,c]H} \mathbf{F}_{[r,b]}^{[k,c]} \mathbf{v}_{j,r}^{[k,c]} \right|^2 \right) \end{aligned} \quad (37)$$

where $\mathbf{u}_{i,G}^{[k,c]}$ and $\mathbf{v}_{i,G}^{[k,c]}$ are the i th columns of the matrices $\mathbf{U}_G^{[k,c]}$ and $\mathbf{V}_G^{[k,c]}$, and also $\mathbf{u}_{i,F}^{[k,c]}$ and $\mathbf{v}_{i,F}^{[k,c]}$ are the i th columns of the matrices $\mathbf{U}_F^{[k,c]}$ and $\mathbf{V}_F^{[k,c]}$, respectively. In the case of perfect IA, each phase of the relay-assisted multi-cell multi-user network is equivalent to the set of $K \times C$ independent MIMO links. In order to avoid inter-stream interference, it is necessary that each effective MIMO channel to be converted to parallel independent subchannels. Thus, in (34) to (37), $\mathbf{V}_G^{[k,c]}$, $\mathbf{U}_G^{[k,c]}$, $\mathbf{V}_F^{[k,c]}$ and $\mathbf{U}_F^{[k,c]}$ must be chosen as

$$\mathbf{V}_G^{[k,c]} = \mathbf{V}_{G,IA}^{[k,c]} \mathbf{V}_{G,SVD}^{[k,c]} \quad (38)$$

$$\mathbf{U}_G^{[k,c]} = \mathbf{U}_{G,IA}^{[k,c]} \mathbf{U}_{G,SVD}^{[k,c]}$$

$$\mathbf{V}_F^{[k,c]} = \mathbf{V}_{F,IA}^{[k,c]} \mathbf{V}_{F,SVD}^{[k,c]} \quad (39)$$

$$\mathbf{U}_F^{[k,c]} = \mathbf{U}_{F,IA}^{[k,c]} \mathbf{U}_{F,SVD}^{[k,c]}$$

where $\mathbf{U}_{G,SVD}^{[k,c]} \in \mathbb{C}^{d \times d}$ ($\mathbf{U}_{F,SVD}^{[k,c]} \in \mathbb{C}^{d \times d}$) and $\mathbf{V}_{G,SVD}^{[k,c]} \in \mathbb{C}^{d \times d}$ ($\mathbf{V}_{F,SVD}^{[k,c]} \in \mathbb{C}^{d \times d}$) are the left and right singular matrices for the effective MIMO channel matrix $\mathbf{U}_{G,IA}^{[k,c]H} \mathbf{G}_c^{[k,c]} \mathbf{V}_{G,IA}^{[k,c]}$ ($\mathbf{U}_{F,IA}^{[k,c]H} \mathbf{F}_{[k,c]}^{[k,c]} \mathbf{V}_{F,IA}^{[k,c]}$) which can be obtained using the singular value decomposition (SVD) as

$$\mathbf{U}_{G,IA}^{[k,c]H} \mathbf{G}_c^{[k,c]} \mathbf{V}_{G,IA}^{[k,c]} = \mathbf{U}_{G,SVD}^{[k,c]} \mathbf{\Sigma}_{c,G}^{[k,c]} \mathbf{V}_{G,SVD}^{[k,c]H} \quad (40)$$

$$\mathbf{U}_{F,IA}^{[k,c]H} \mathbf{F}_{[k,c]}^{[k,c]} \mathbf{V}_{F,IA}^{[k,c]} = \mathbf{U}_{F,SVD}^{[k,c]} \mathbf{\Sigma}_{c,F}^{[k,c]} \mathbf{V}_{F,SVD}^{[k,c]H} \quad (41)$$

where $\mathbf{\Sigma}_{c,G}^{[k,c]}$ ($\mathbf{\Sigma}_{c,F}^{[k,c]}$) is the singular value matrix for the effective MIMO channel matrix.

APPENDIX B CALCULATION OF (26)

Similar to the AF scheme, by assuming i.i.d. Gaussian signaling, the achievable sum rate for the DF scheme given in (26) can be rewritten as

$$R_{DF}^{\Sigma} = \frac{1}{2} \sum_{c=1}^C \sum_{k=1}^K \sum_{i=1}^d \log_2 \left(1 + \Psi_{i,DF}^{[k,c]} \right) \quad (42)$$

where $\Psi_{i,DF}^{[k,c]}$ is the SINR of the i th received stream corresponding to the second phase of the protocol.



This parameter can be computed as $\Psi_{i,F}^{[k,c]}$ in (37). Similar to the AF case, for the DF scheme, the precoding and postcoding matrices can be obtained as (39) and (41).

APPENDIX C DERIVATION OF THE DoF

Substituting (26) into (27), the DoF at MS^[k,c] can be computed as [15]

$$\begin{aligned} d_{DF}^{[k,c]} &= \lim_{P \rightarrow \infty} \frac{R_{DF}^{[k,c]}}{\log_2(P)} \\ &= \frac{1}{2} \lim_{P \rightarrow \infty} \left\{ \frac{1}{\log_2(P)} \log_2 \det[\mathbf{I}_d + (\sigma_n^2 \mathbf{I}_d \right. \\ &\quad \left. + \mathbf{J}_F^{[k,c]} \mathbf{J}_F^{[k,c]H})^{-1} \mathbf{S}_F^{[k,c]} \mathbf{S}_F^{[k,c]H}] \right\} \\ &= \frac{1}{2} \left[\lim_{P \rightarrow \infty} \left\{ \frac{1}{\log_2(P)} \log_2 \det[(\sigma_n^2 \mathbf{I}_d \right. \right. \\ &\quad \left. \left. + \mathbf{J}_F^{[k,c]} \mathbf{J}_F^{[k,c]H})^{-1} \mathbf{S}_F^{[k,c]} \mathbf{S}_F^{[k,c]H}] \right\} \right]^+ \\ &= \frac{1}{2} \left[\lim_{P \rightarrow \infty} \left(\frac{\log_2 \det[\mathbf{S}_F^{[k,c]} \mathbf{S}_F^{[k,c]H}]}{\log_2(P)} \right. \right. \\ &\quad \left. \left. - \frac{\log_2 \det[\sigma_n^2 \mathbf{I}_d + \mathbf{J}_F^{[k,c]} \mathbf{J}_F^{[k,c]H}]}{\log_2(P)} \right) \right]^+ \\ &= \frac{1}{2} \left[\lim_{P \rightarrow \infty} \left(\frac{\sum_{i=1}^{\text{rank}(\mathbf{S}_F^{[k,c]})} \log_2(\lambda_i(\mathbf{S}_F^{[k,c]} \mathbf{S}_F^{[k,c]H}))}{\log_2(P)} \right. \right. \\ &\quad \left. \left. - \frac{\sum_{i=1}^{\text{rank}(\mathbf{J}_F^{[k,c]})} \log_2(\lambda_i(\mathbf{J}_F^{[k,c]} \mathbf{J}_F^{[k,c]H}) + \sigma_n^2)}{\log_2(P)} \right) \right]^+ \\ &= \frac{1}{2} \left[\lim_{P \rightarrow \infty} \left(\frac{\sum_{i=1}^{\text{rank}(\mathbf{S}_F^{[k,c]})} \log_2(\mathbf{S}_{F,i}^{[k,c]} \mathbf{S}_{F,i}^{[k,c]H})}{\log_2(P)} \right. \right. \\ &\quad \left. \left. - \frac{\sum_{i=1}^{\text{rank}(\mathbf{J}_F^{[k,c]})} \log_2(\mathbf{J}_{F,i}^{[k,c]} \mathbf{J}_{F,i}^{[k,c]H} + \sigma_n^2)}{\log_2(P)} \right) \right]^+ \\ &= \frac{1}{2} \left[\lim_{P \rightarrow \infty} \left(\frac{\sum_{i=1}^{\text{rank}(\mathbf{S}_F^{[k,c]})} \log_2(P c_{i,S})}{\log_2(P)} \right. \right. \\ &\quad \left. \left. - \frac{\sum_{i=1}^{\text{rank}(\mathbf{J}_F^{[k,c]})} \log_2(P c_{i,J} + \sigma_n^2)}{\log_2(P)} \right) \right]^+ \\ &= \frac{1}{2} \left[\lim_{P \rightarrow \infty} \left(\frac{\sum_{i=1}^{\text{rank}(\mathbf{S}_F^{[k,c]})} \log_2(P)}{\log_2(P)} \right) \right]^+ \end{aligned}$$

$$\begin{aligned} &\left. - \frac{\sum_{i=1}^{\text{rank}(\mathbf{J}_F^{[k,c]})} \log_2(P)}{\log_2(P)} \right) \right]^+ \\ &= \frac{1}{2} [\text{rank}(\mathbf{S}_F^{[k,c]}) - \text{rank}(\mathbf{J}_F^{[k,c]})]^+ \end{aligned}$$

where $\mathbf{S}_{F,i}^{[k,c]}$ and $\mathbf{J}_{F,i}^{[k,c]}$ are the i th rows of $\mathbf{S}_F^{[k,c]}$ and $\mathbf{J}_F^{[k,c]}$, respectively. Also $c_{i,S}$ and $c_{i,J}$ are two constant values, where $0 < c_{i,S} \ll +\infty$ and $0 < c_{i,J} \ll +\infty$.

REFERENCES

- [1] C. Suh, M. Ho, and D. N. C. Tse, "Downlink interference alignment," *IEEE Trans. Commun.*, vol. 59, no. 9, pp. 2616–2626, Sep. 2011.
- [2] K. T. Truong, P. Sartori, and R. W. Heath, "Cooperative algorithms for MIMO amplify-and-forward relay networks," *IEEE Trans. Signal Process.*, vol. 61, no. 5, pp. 1272–1287, Mar. 2013.
- [3] V. Cadambe and S. Jafar, "Interference alignment and degrees of freedom of the K -user interference channel," *IEEE Trans. Inf. Theory*, vol. 54, no. 8, pp. 3425–3441, Aug. 2008.
- [4] W. Shin, N. Lee, J.-B. Lim, C. Shin, and K. Jang, "On the design of interference alignment scheme for two-cell MIMO interfering broadcast channels," *IEEE Trans. Wirel. Commun.*, vol. 10, no. 2, pp. 437–442, Feb. 2011.
- [5] K. T. K. Cheung and L. Hanzo, "Distributed energy spectral efficiency optimization for partial/full interference alignment in multi-user multi-relay multi-cell MIMO systems," *IEEE Trans. Signal Process.*, vol. 64, no. 4, pp. 882–896, Feb. 2016.
- [6] A. S. Zamzam, A. El-Keyi, M. Nafie, and Y. Mohasseb, "On the degrees of freedom of the two-cell two-hop MIMO network with dedicated and shared relays," *IEEE Trans. Wirel. Commun.*, vol. 14, no. 12, pp. 6738–6751, Dec. 2015.
- [7] X. Li, H. Al-Shatri, R. S. Ganesan, D. Papsdorf, A. Klein, and T. Weber, "Uplink-downlink duality of interference alignment in cellular relay networks," in *Proc. 10th Int. ITG Conf. on Systems, Commun. and Coding*, Hamburg, Germany, Feb. 2015, pp. 1–6.
- [8] X. Wang, Y. P. Zhang, P. Zhang, X. Ren, "Relay-aided interference alignment for MIMO cellular networks," in *Proc. Int. Symp. on Inf. Theory (ISIT)*, Cambridge, MA, USA, July 2012, pp. 2641–2645.
- [9] C. D. T. Thai, J. Lee, H. X. Nguyen, M. Berbineau, and T. Q. S. Quek, "Multi-cell multi-user relaying exploiting overheard signals," *IEEE Wirel. Commun. Lett.*, vol. 3, no. 4, pp. 401–404, Aug. 2014.
- [10] Y. Shu, Q. Wang, J. Zhang, and T. Sun, "Relay-aided interference alignment and neutralization for 3-cellular interference channels," in *Proc. IEEE/CIC Int. Conf. on Commun. in China (ICCC)*, Shanghai, China, Oct. 2014, pp. 637–641.
- [11] D. A. Basnayaka and H. Haas, "Overcoming large-scale fading in cellular systems with network coordination," *IEEE Trans. Commun.*, vol. 62, no. 7, pp. 2589–2601, Jul. 2014.
- [12] Q. F. Zhou, F. C. M. Lau, and S. F. Hau, "Asymptotic analysis of opportunistic relaying protocols," *IEEE Trans. Wirel. Commun.*, vol. 8, no. 8, pp. 3915–3920, Aug. 2009.
- [13] J. Tang and S. Lambotharan, "Interference alignment techniques for MIMO multi-cell interfering broadcast channels," *IEEE Trans. Commun.*, vol. 61, no. 1, pp. 164–175, Jan. 2013.
- [14] S. Liu, Y. Du, "A general closed-form solution to achieve interference alignment along spatial domain," in *Proc. IEEE Global Commun. Conf. (GLOBECOM)*, Miami, USA, Dec. 2010, pp. 1–5.
- [15] D. S. Papailiopoulos and A. G. Dimakis, "Interference alignment as a Rank constrained rank minimization," *IEEE Trans. Signal Process.*, vol. 60, no. 8, pp. 4278–4288, Aug. 2012.



- [16] B. Zhuang, R. A. Berry, and M. L. Honig, "Interference alignment in MIMO cellular networks," in *Proc. IEEE ICASSP*, Prague, Czech Republic, May 2011, pp. 3356–3359.
- [17] S. A. Jafar, M. J. Fakhreddin, "Degrees of Freedom for the MIMO Interference Channel," *IEEE Trans. Inf. Theory*, vol. 35, no. 7, pp. 2637–2642, July 2007.
- [18] T. Gou and S. A. Jafar, "Degrees of Freedom of the K -User $M \times N$ MIMO Interference Channel", *IEEE Trans. Inf. Theory*, vol. 56, no. 12, pp. 6040–6057, Dec. 2010.



Ali Golestani received his B.Sc. degree in electrical engineering from IHU, Tehran, Iran, in 2012 and the M.Sc. degree in electrical engineering from K. N. Toosi University of Technology, Tehran, Iran, in 2015. His research interests include cooperative communications, interference alignment (IA) technique, and new generation cellular networks technologies.



Ali H. Bastami received his B.Sc. degree in electrical engineering from the University of Science and Technology, Tehran, Iran, in 2003, the M.Sc. degree (with highest honors) in electrical engineering from Amir-Kabir University of Technology, Tehran, Iran, in 2006, and the Ph.D. degree in electrical engineering from the University of Tehran, Tehran, Iran, in 2011. Since 2012, he has been an Assistant Professor at the Department of Electrical and Computer Engineering, K. N. Toosi University of Technology, Tehran, Iran. He received the best thesis award from the Department of Electrical and Computer Engineering, University of Tehran, in 2011. His research interests include cooperative communications, cognitive radio networks and multiple-input multiple-output (MIMO) communication systems.



K. Mohamed-pour was born in 1954, and received his B.Sc. and M.Sc. degrees in Electrical Engineering-Telecommunication in Tehran, 1979 and 1987 respectively. After some lecturing in Communication department in Electrical Engineering Faculty of K.N.Toosi University of Technology, continued his studying towards Ph.D. in University of Manchester, U.K. 1995. Dr. Mohamed-pour is a full professor at K.N.Toosi University and has published several books in Digital Signal Processing and Digital Communications. His main research interests are Broadband Wireless Communications, MIMO-OFDM, and Communication Networks.

